Chemical Geology 169 (2000) 449–460

CHEMICAL GEOLOGY
INCLUDING
ISOTOPE GEOSCIENCE

www.elsevier.com/locate/chemgeo

Recent calcite spar in an aquifer waste plume: a possible example of contamination driven calcite precipitation

K.J. Tobin [a,*], F.S. Colwell [b], T.C. Onstott [a], R. Smith [b]

[a] Department of Geosciences, Princeton University, Princeton, NJ 08544 USA
[b] Biotechnologies Department, Idaho National Engineering and Environmental Laboratory, Idaho Falls, ID 83415 USA

Received 28 April 1999; accepted 29 November 1999

Abstract

This paper documents possible modern (within the last 50 years) calcite cementation within an unconfined contaminated aquifer at the Test Area North (TAN) on the Idaho National Engineering and Environmental Laboratory site. Inferred modern calcite occurs at the distal tips of the latest generation of calcite cement and has bright luminescence when examined by cathodoluminescence. Luminescent distal tips have elevated Mn values (up to 6400 ppm) when compared with other TAN calcite cement (< 200 ppm). Additionally, speciation modeling with PHREEQE indicates that modern TAN groundwater exhibits a slight supersaturation with respect to calcite (calculated saturation indexes range from 0.2 to 0.5). The observed abundance of luminescent distal tips (< 1–38 μg calcite/g total sample) is significantly less than the potential calcite precipitation (250–1100 μg calcite/g total sample) indicated by laboratory microbial activity measurements; a finding consistent with previous studies. Finally, while our results do not elucidate the specific mechanism(s) responsible for the elevated Mn present in some TAN calcite, we do demonstrate at least an indirect microbial involvement for Mn enrichment. Therefore, it is conceivable that geochemical signatures indicative of distinctive redox conditions can be recognized in recently formed calcite from other contaminated groundwater systems. © 2000 Elsevier Science B.V. All rights reserved.

Keywords: Calcite; Test Area North; Precipitation Aquifer

1. Introduction

The microbial biomass and diversity of the terrestrial subsurface has been documented in many recent reports (see Amy and Haldeman, 1997). Far less is known about the level of microbial activity and cellular turnover. A combination of mass balance and ground water dating suggest that the microbial respiration rates (i.e., CO_2 production) for confined aquifers are orders of magnitude less than that found in the soil zone (e.g., Chapelle and Lovley, 1990; Phelps et al., 1994). Similar estimates have been reported for the same aquifers by assuming that diagenetic carbonates were the product of ongoing subsurface microbial activity (e.g., McMahon et al.,

---

[*] Corresponding author. University of Illinois at Chicago, Department of Earth and Environmental Sciences, M/C 186, 845 W. Taylor St., Chicago, IL, 60607 USA. Tel. +1-312-413-0098; fax: +1-312-413-2279.

E-mail address: kjtobin@uic.edu (K.J. Tobin).

PII: S0009-2541(00)00220-5

1990). Authigenic carbonate may reflect precipitation in geologically ancient, near-surface environments and unequivocal proof of modern, subsurface, formation is difficult to establish.

The study of mineral dissolution and precipitation in contaminated aquifers (e.g., Hiebert and Bennett, 1992) provides an alternative approach to estimate subsurface microbial activity where the geochemical environment has been dramatically altered (e.g., reduction in Eh) over a documented time interval. Multiple lines of self-consistent evidence (relative timing, textures indicative of specific diagenetic environments, mineral geochemistry) can be used to distinguish ancient from recent calcite associated with the modern, contaminated aquifer. This paper outlines such a set of corroborative observations that supports a modern origin for some calcite cements present in the contaminated aquifer at Test Area North (TAN) on the Idaho National Engineering and Environmental Laboratory (INEEL) site.

A secondary question revolves around whether this modern calcite formed by nucleation associated with microbial activity (Coleman et al., 1993; Vasconcelos et al., 1995) or reflects inorganic precipitation from fluids whose chemistry reflect the impact of microbial processes. Carbonate with spatial variations in Mn and Fe concentrations indicative of a progression from Mn^{4+} to Fe^{3+} to SO_4^{2-} reduction have been described from a variety of marine depositional settings (Pigott and Land, 1986; Sansone et al., 1990; Hendry, 1993; Tribble, 1993; Tobin et al., 1996). While, at present, we can offer no evidence to support a direct microbial origin for modern TAN calcite we do suggest that the elevated Mn content of some TAN calcite reflects a proxy for localized oxygen consumption that is still observed today within the contaminated aquifer at TAN.

2. TAN site geology and hydrogeology

The Snake River Plain Aquifer (SRPA) lies beneath the INEEL and consists of a series of saturated basalt flows and interbedded, poorly consolidated sedimentary and pyroclastic deposits. The basalt beneath TAN is a typical tholeiitic basalt that exhibits a wide range of lithologic textures and structures. Subsurface basalt samples from TAN range from being fresh gray dense and massive to orange–red oxidized, highly vesicular, and highly fractured. The basalt samples consist of phenocrysts of olivine, plagioclase, clinopyroxene, titanomagnetite, ilmenite, and rare apatite present in a glassy groundmass. Minor secondary minerals occur in the vesicles and fractures of TAN basalts (mostly calcite with minor calcareous Al silicate, microcrystalline silica, and pyrite; Rightmire and Lewis, 1987). Numerous sedimentary interbeds are also encountered in the TAN subsurface, with two interbeds (P–Q interbed and Q–R interbed) consistently correlated between boreholes.

The focus of this study was on basaltic core samples from TAN, boreholes 33 and 37 at intervals between the P–Q and Q–R interbeds. TAN-33 core samples were obtained in late 1996 and TAN-37 samples in the middle of 1997. K–Ar dating suggests that basalts from this interval range in age from 1.2 to 1.4 Ma (Lamphere et al., 1994). Additional basalt cores from between the P–Q and Q–R interbeds obtained from other boreholes at TAN were examined (TAN boreholes 34 and 48, TCH-1, TCH-2, GIN-5).

The topmost core samples from boreholes 33 and 37 occur immediately below the water table (at TAN the water table is located at 59–69 mbsl; Anderson and Bowens, 1995). Groundwater flow direction in the SRPA is generally from the northeast to the southwest. However, in the vicinity of TAN, the potentiometric surface (water table) is notably flat and the direction of groundwater movement is generally from north to south. Because of the flat potentiometric surface, the local flow direction varies seasonally and is affected by the pumping of TAN production boreholes. Rates of groundwater movement in the TAN vicinity range between 0.0006 and 1.3 m/day (Kaminsky et al., 1994).

3. TAN aquifer geochemistry

The interval between the P–Q and Q–R interbeds at TAN defines an unconfined aquifer that contains a variety of contaminants including trichloroethylene (TCE), industrial sewage, and radionuclides such as

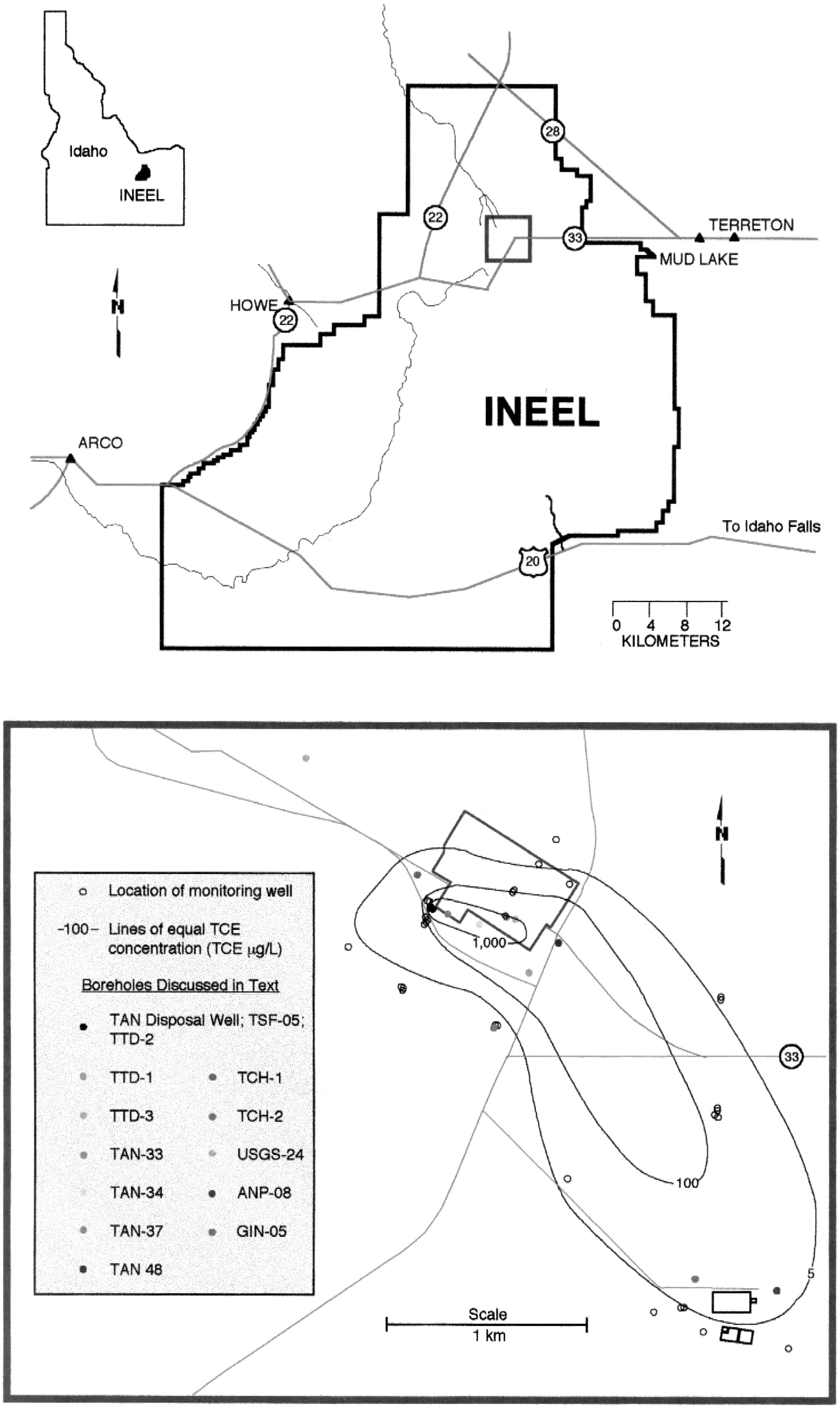

Fig. 1. Locality map showing location of TCE plume at TAN with position of boreholes mention in text illustrated. Light gray lines indicate roads and the TAN site is outlined in dark gray.

^{60}Co and ^{90}Sr. At the TAN Disposal Well TCE concentrations as high as 35,000 μg/l have been measured as recently as 1987 (Mann and Knobel, 1987), which forms the point source for the TCE plume present at TAN (Fig. 1). More recently (Colwell et al., unpublished data, 1996) TCE values of 24,000 μg/l have been measured close to the TAN Disposal Well at borehole TSF-05. The closest borehole to the TAN Disposal Well from which basalt samples were examined in this study is TAN-37, which has TCE concentrations of 5000 μg/l (Colwell et al., unpublished data, 1997). Lower TCE concentrations have been measured from boreholes 34 (Wylie et al. 1999; 1000 μg/l), 33 (Lehman et al., 1999; 500 μg/l), and 48 (Lehman et al., 1999; 200 μg/l) that are located further away from the TAN Disposal Well than TAN 37 (Fig. 1). Finally, TCE values from boreholes near the leading edge of the plume are quite low (e.g., GIN-5; Fig. 1).

Dissolved oxygen (DO) measurements exhibit an antithetical spatial variation when compared with TCE. For example, DO value of 10 mg/l (Knobel et al., 1992) has been measured in borehole ANP-08, which is located at the southern terminus of the TCE plume (Fig. 1). Additionally, to the north of the plume at TTD-03, recorded DO is similarly high (9 mg/l; Knobel et al., 1992). DO concentrations of 7–9 mg/l are typical of the SRPA outside of TAN (Wood and Low, 1986). However, within the plume, DO values are significantly lower and decrease progressively toward the TAN Disposal Well. At borehole USGS-24 DO = 6 mg/l (Knobel et al., 1992). Proximal to USGS-24, a later drilled borehole (TAN-33) has a similar DO value (Colwell et al., unpublished data, 1996; 6 mg/l). Closer to the TAN Disposal Well at TAN-37, even lower values for DO exist (Colwell et al., unpublished data, 1997; 3 mg/l). Finally, at the TAN Disposal Well DO is below detection limit (<1 mg/l; Knobel et al., 1992; Sorenson et al. 1999).

Groundwater Mn values exhibit significant spatial variations. Knobel et al. (1992) document elevated Mn at the TAN Disposal Well (84 μg/l) when compared with ANP-08, located toward periphery of the TCE plume (Fig. 1), which was below detection limit (1 μg/l). Likewise, Colwell et al. (unpublished data, 1996) document elevated Mn values (up to 76 μg/l) immediately adjacent to the TAN Disposal Well at TSF-05 (Fig. 1). Relatively low Mn values (≤ 20 μg/l) are present in water from most of the other boreholes at TAN.

4. Summary of TAN microbiology

Microbial biomass in the basalt from the corehole at intermediate distance from the TAN Disposal Well (TAN-33) was at the limit of detection for most assays and minimal ^{14}C-acetate mineralization was detected from samples (Lehman et al., 1998). Culturable aerobic oligotrophic heterotrophs, phenol-oxidizers, and methanotrophs were detected at concentrations of $0–10^4$, $<10^2$, and <20 cells/g, respectively. Dissimilatory iron-reducing bacteria were evident in only 25% of the cores. The low numbers of culturable cells in the cores from TAN-33 is consistent with previous studies of the numbers of microorganisms in minimally contaminated (TAN-48; Lehman et al., 1999) or uncontaminated areas of the SRPA (Colwell, 1989; Colwell and Lehman, 1997; Palumbo et al. 1994).

In contrast, basalt from TAN-37, a borehole proximal to the TAN Disposal Well, showed measurable biomass by phospholipid fatty acid analysis (ca. 3 pmol/g) and much higher levels of acetate mineralization (Lehman et al., 1999). Higher numbers of the different physiological types of microorganisms were enriched in all samples from TAN-37 relative to those from TAN-33. The following order of prevalence was discernible in enumerations of specific microbial types in cores from TAN-37: phenol oxidizers ($<10^5$ cells/g) > propanotrophs ($<10^4$ cells/g) ≫ methanotrophs ($<10^2$ cells/g) ≫ nitrifiers. Dissimilatory iron-reducing bacteria were evident in 75% of the cores from TAN-37.

Microbial DNA was extracted from selected TAN-33 and TAN-37 samples and amplified using PCR with eubacterial and archaeal primers. TAN-33 samples did not yield visible PCR bands; however, extractions from selected TAN-37 samples indicated higher levels of DNA (Lehman et al. 1999). Eubacterial PCR bands were recovered from all of the TAN-37 samples that were amplified except the combusted basalt control. Only one of the 10 samples yielded an archaeal PCR band. Cloning and sequencing of these PCR bands indicate a diversity of eubacterial microorganisms in the samples from the top of the aquifer in TAN-37 including types that are common in soil environments (e.g., *Acinetobacter*, *Pseudomonas*, and actinomycetes).

Comparison of the data from TAN-33 and TAN-37 indicate that bacteria associated with basalt may be present in low numbers in pristine areas of the aquifer while a substantial stimulation of similar types of organisms may result from organic contamination. The close proximity of TAN-37 to the original injection borehole for the waste relative to other studied TAN boreholes is the most likely explanation for the higher microbiological activities in TAN-37 samples.

5. Methods

Polished thin sections (2.5 × 5.0 cm) were examined in detail in transmitted light and cathodoluminescence (CL) using a Nuclide luminoscope (voltage = 8 kV, beam current = 500 μA, and chamber pressure = 60–90 mTorr). CL microscopy of thin sections was used to select areas for electron microprobe (EMP) analysis and CL of analyzed areas also was verified after EMP analysis. Images of CL bands were captured using a cooled, three-chip, charge-coupled device (CCD) camera (Optronics DEI-750; Goleta, CA, USA) and dimensional analysis of these bands was performed with Image-Pro® Plus 3.0 (Media Cybernetics; Silver Spring, MD, USA).

Calcite samples for inductively coupled plasma (ICP), stable isotope ratio (SIR), and accelerator mass spectrometry (AMS) analysis were obtained by drilling areas on thin section billets, matched to accompanying thin sections, with a microscope-mounted microdrill. Samples with mass > 100 mg were drilled to form a powder for use in ICP analyses that were completed commercially at Actilabs. Smaller mg-to-sub-mg sized samples were also drilled and a powder collected for SIR and AMS analysis that were performed at Mountain Mass Spectrometry (MMS) and PRIME Labs, respectively. Groundwater samples were obtained from a multi-level sampler deployed in the TAN-33 borehole for 6 months for analysis of dissolved inorganic carbon (DIC) δ^{13}C (MMS).

Wavelength dispersive EMP analysis for Mg, Ca, Mn, Fe, and Sr in calcite was performed on polished thin sections using a Cameca SX-50 Electron Microprobe (Princeton Material Institute). Operating conditions included an accelerating voltage of 20 kV, a beam current of 20 nA, and a defocused beam of 5 μm in width to minimize sample volatilization. Count times were as follows: Ca = 10 s; Mg, Mn, and Fe = 90 s; and Sr = 70 s with corresponding 2σ detection limits of Mg = 0.08 wt.% $MgCO_3$; Mn = 200 ppm; Fe = 300 ppm; and Sr = 500 ppm.

6. Results

6.1. Petrography of vesicle filling phases

In order to put possible modern calcite into an overall historical context, it is necessary to characterize the petrography of all vesicle filling phases. A variety of calcite and non-calcite phases occlude the vesicles and fractures of the TAN aquifer whose relative timing of formation (or paragenetic) relationships are shown in Fig. 2. Calcite is both micritic/microspar and sparry in form. The initial generation of sparry calcite has a non-drusy fabric consisting of either equant or columnar cement. First generation columnar calcite is characterized by having obtuse crystal terminations and fluid inclusions most of which are all-liquid and primary. Fine-grained carbonate exhibits preserved rhizoliths, massive micritic/microsparic crusts, and micritic clasts

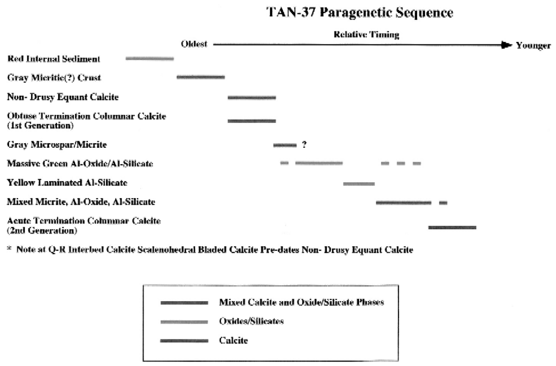

Fig. 2. Paragenetic sequence showing relative timing relationships between major diagenetic phases present in TAN-37.

with circumgranular cracking. Micritic/microspar post-dates the first generation of sparry calcite. Mixed carbonate/silicate/oxides also post-date first generation sparry calcite and are locally interlayered with second generation sparry calcite. Second generation sparry cement consists of columnar calcite with acute crystal terminations. Calcite generations are either gradational with each other or are separated by distinct layer(s) consisting of various non-carbonate phases (Fig. 2).

Nearly all of the calcite spar has a faint blue luminescence except in three samples from TAN-37 where the distal tips of second generation columnar calcite crystals are bright luminescent (Fig. 3). Bright luminescent tips are very thin (<20 μm wide) and have a very low abundance (<1–38 μg calcite/g total sample, as determined by image dimensional analysis). For the sample with <1 μg calcite/g total sample, it was determined by image analysis that bright luminescent calcite occupied an area equal to 600 μm^{-2} in a sample whose overall area equals 13.609 cm^{-2}; note that pixel resolution was ≈ 4 μm. In some instances, bright luminescent calcite is followed by a secondary thin band of blue luminescent calcite.

6.2. Calcite minor element composition

The minor element composition of calcite, specifically Mn and Fe contents, varies depending on redox state of the diagenetic fluids from which these cements formed. Calcite minor element compositions were determined using in situ (EMP) and bulk (ICP) methods. First generation sparry calcite was determined by EMP to have Mg ranging from 0.36 to 0.44 wt.% ($n=3$) with both Mn and Fe below detection limit. Second generation columnar calcite has Mg = 0.10–0.94 wt.% ($n=60$) as determined by EMP. Three cathodoluminescent categories of second generation calcite were subjected to in situ analysis: initial blue luminescent, bright luminescent, secondary blue luminescent. Most analyses of initial blue luminescent calcite were below detection for Mn (54 out of 55; with one analysis at the detection limit, 200 ppm) and Fe (52 out of 55; with two analyses at the detection limit, and another at 400 ppm). Bright luminescent calcite ranges from 200 to 6400 ppm in Mn ($n=4$) with Fe below detection limit. Secondary calcite with blue luminescence have Mn and Fe below the detection limit ($n=1$). All calcite analyzed has Sr below detection limit (500 ppm).

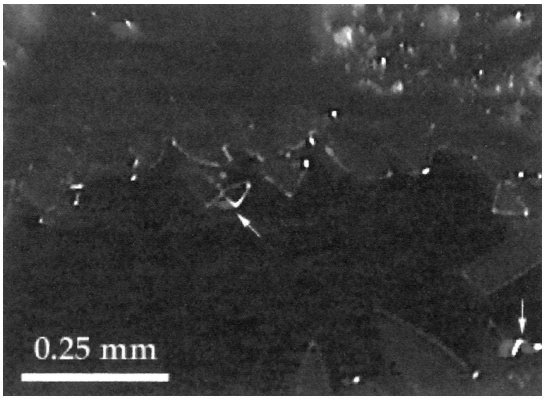

Fig. 3. Cathodoluminescence photomicrograph of the bright luminescent tips (arrow) of second generation columnar calcite from TAN-37, which has a general faint blue luminescence.

Elemental compositions for first and second generation calcite spar were also determined by ICP ($n=2$ and 3, respectively) and are consistent with EMP results. Mg values determined with ICP for first and second generation calcite overlap with values determined by EMP (first = 0.34–0.41 wt.%, second = 0.28–0.34 wt.%). Likewise, Mn, Fe, and Sr values determined by ICP are consistent with the below detection limit EMP analyses of initial blue luminescent calcite. First and second generation calcite have similar concentrations of Mn (first = 6–13 ppm, second = 4–15 ppm), Fe (first and second = 40–70 ppm), and Sr (first = 40–47 ppm, second 22–49 ppm). Other significant trace elements in calcite determined by ICP include Na, Cd, and Ba with values for first and second generation calcite spar that are similar (Na, first = 80–130 ppm, second = 60–150 ppm; Cd, first and second <2 ppm; Ba, first = 22–27 ppm, second = 17–22 ppm).

6.3. Calcite $\delta^{13}C$ and $\delta^{18}O$ values

Stable isotopic values from calcite were obtained from both whole-rock material and discrete phases from TAN-33 and TAN-37 boreholes to see if any of these phases could have been precipitated in equilibrium with modern groundwater. These phases include micrite/microspar and several types of sparry calcite including equant calcite (filling both vugs and fractures) and two generations of columnar calcite. With the exception of some TAN-37 vein calcite from the Q–R interbed, the δ^{13}C and δ^{18}O values of all of the above phases overlap (Figs. 4 and 5). The δ^{13}C and δ^{18}O values from TAN-33 calcite range from −3.07‰ to −6.89‰ (avg. = −4.77‰) and −12.01‰ to −17.62‰ (avg. = −14.99; $n = 55$), respectively. Calcite from TAN-37, without interbed vein calcite, yields δ^{13}C and δ^{18}O range from −2.98‰ to − 7.19‰ (avg. = −5.47‰) and −12.44‰ to −18.32‰ (avg. = −14.64‰; $n = 35$), respectively. Q–R interbed vein calcite from TAN 37 has slightly more negative δ^{13}C (−6.99‰ to −8.83‰, avg. = −7.92‰; $n = 4$; Fig. 5).

6.4. Water δ^{13}C DIC values

The δ^{13}C of DIC in groundwater equilibrated for 6 months within a multi-level sampler deployed in TAN-33 borehole was used to determine the plausibility of TAN calcite formation from modern groundwater. Overall values range from −10.0‰ to −11.9‰ (avg. = −10.6‰, $n = 53$) with most values between −10.0‰ and − 10.6‰.

6.5. Carbon-14 activity from TAN 37 calcite cement

Two samples of calcite cement from TAN-37 were analyzed for ^{14}C by AMS to determine the age

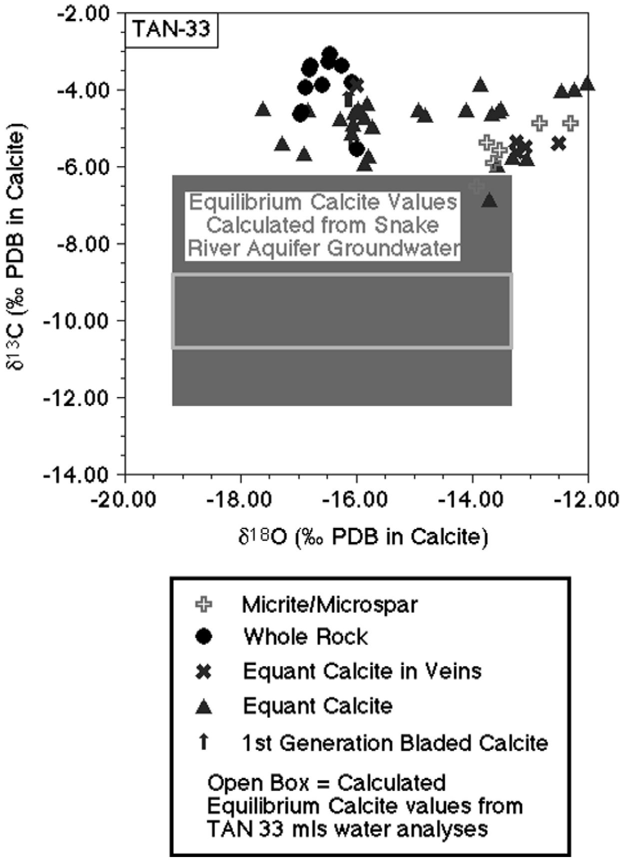

Fig. 4. δ^{13}C and δ^{18}O cross-plots from whole-rock and discrete calcite phases from TAN-33. Shaded equilibrium field based on groundwater data from Wood and Low (1986).

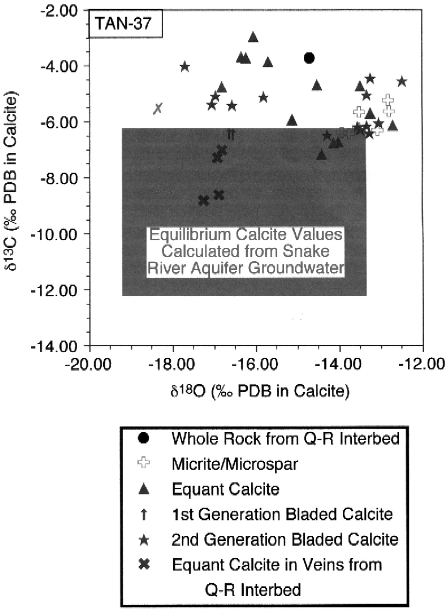

Fig. 5. δ^{13}C and δ^{18}O cross-plots from whole-rock and discrete calcite phases from TAN-37. Shaded equilibrium field based on groundwater data from Wood and Low (1986).

of the carbon present in TAN calcite cement. The latest generation of calcite cement was analyzed from a basalt and Q–R sedimentary interbed sample. For these samples, the concentration of ^{14}C atoms is 0.6 ± 1.4 and 0 ± 1.3 per 10^{-15} atoms of total carbon, which is below detection limit.

7. Origin of tan calcite cements

7.1. Ancient calcite cements

The presence of rhizoliths, massive micritic/microsparic crusts, and micritic clasts with circumgranular cracking are characteristic of carbonate formation in a meteoric diagenetic setting (James and Choquette, 1984). As previously noted, the basalts examined in this study are within the phreatic zone, implying an ancient origin for the observed vadose features.

Corroborating evidence supporting the assertion that most calcite has an ancient, vadose origin is that the calcite δ^{13}C isotopic values are mostly not in the range consistent with equilibrium formation from modern groundwater. All calcite phases examined from TAN-33 lie outside equilibrium values calculated from DIC determinations.

Equilibrium calcite values are determined based on δ^{13}C of DIC. These equilibrium values are calculated using temperatures ranging from 10 to 15°C; a pH of 8, which is an average for groundwater in the TAN area (Knobel et al., 1992); and using the equilibrium fractionation factors of Romanek et al. (1992).

Based on the above parameters, equilibrium calcite must be fractionated in δ^{13}C by $+1.2$‰ from observed TAN-33 DIC values (or -8.8‰ to 10.7‰). Calculated equilibrium values are clearly more negative than measured calcite δ^{13}C values from various TAN-33 carbonate phases (Fig. 4). Considering more geographically widespread sites throughout the eastern SRPA (Wood and Low, 1986), a wider range of DIC δ^{13}C values and hence a wider range of calculated calcite δ^{13}C values are determined. Even with the expansion of the equilibrium field, most observed calcite values plot outside this field (Figs. 4 and 5). Calcite δ^{13}C values from TAN overlap with vadose calcite compositions from elsewhere in the SRPA (Rightmire and Lewis, 1987; Conrad et al., 1997).

Additional supporting evidence is the positive δ^{18}O values for some TAN calcite cements. Some of these values are more positive than can be accounted for by equilibrium precipitation from modern groundwater, suggesting the influence of near surface evaporation. The non-detectable ^{14}C activity measured from latest generation calcite cements also supports an ancient origin for these cements. The negative δ^{13}C values of the Q–R interbed vein calcite (Fig. 5) probably reflect formation in an ancient phreatic setting. Isotopic characterization methods used in this study are not in situ; however, and consequently, these results do not rule out the possible existence of minor quantities of modern calcite.

7.2. Geochemical conditions associated with ancient TAN calcite

Almost all calcite cement examined from TAN has a faint blue luminescence (Fig. 3). Blue luminescence in calcite is believed to be the intrinsic CL color of calcite caused by the presence of lattice defects (Machel et al., 1991) in calcite that is essentially pure and lacks CL activators and quenchers (Amieux et al., 1989). Blue luminescence has been described in Iceland spar (Sippel and Glover, 1965), unaltered Holocene marine calcite cement (Amieux et al., 1989), and in Jurassic marine neomorphic spars (Hendry et al., 1995). Non-activation of CL in intrinsic blue luminescent calcite indicates low Mn concentrations (≤ 15–30 ppm) based on previous CL activator studies (Machel et al., 1991; Savard et al., 1995). Bulk ICP analyses of first and second generation TAN calcite cements yield values for Mn (4–15 ppm) that are consistent with non-activation of CL in TAN cements. Such low concentrations of Mn (and Fe) in TAN cements is consistent with a formation in a vadose or unconfined phreatic zone that was in equilibrium with the overlying atmosphere. The SRPA is open with respect to diffusion from the atmosphere and is always near saturation with respect to DO in areas away from TCE contamination (Wood and Low, 1986).

7.3. Possible modern calcite cements

Today, sub-oxic to anoxic conditions are present within the TCE plume at TAN. Additionally, the distal tips of the latest generation of calcite cement are distinct from preceding cement in their CL and minor element chemistry. Specifically, some distal tips have a bright luminescence (Fig. 3) with elevated Mn values. Therefore, it is reasonable to suggest that the bright luminescent distal tips formed under different geochemical conditions than the vast majority of TAN cement. Additionally, since the bright luminescent distal tips form the most recent material that has precipitated into the porosity present in the TAN basalts it is possible that these tips reflect modern calcite cementation associated with the sub-oxic to anoxic conditions that are currently present at TAN.

Elevated Mn in calcite is consistent with equilibrium precipitation from a Mn-rich fluid as shown below. In groundwater at two disposal boreholes (TAN Disposal Well; TDD-2) measured Mn and Ca concentrations are 0.084 and 0.017 ppm and Ca is 57 and 71 ppm, respectively (Knobel et al., 1992). Dromgoole and Walter (1990) experimentally determined the distribution coefficient (DMn^{2+}) for the partitioning of Mn^{2+} into calcite. They calculated a $DMn^{2+} = 11.7$ at 10°C and at a calcite precipitation rate of 1 μmol m^{-2} h^{-1}; these parameters are most comparable to the conditions associated with calcite precipitation in the TAN aquifer. From this information, we determined that with equilibrium precipitation of calcite from disposal borehole fluids that the Mn in the calcite should be 1100–6900 ppm, which closely compares with the Mn concentration of bright luminescent calcite where $Mn = 200$–6400 ppm. These Mn values are not typical of calcite formed from oxic meteoric water outside the TCE plume as discussed previously.

A salient question is whether calcite is thermodynamically favored to be precipitated from modern TAN groundwater? Speciation modeling (PHREEQE) addresses the above question. Input parameters include the measured cation and anion concentrations, pH, and temperatures of waters from four wells proximal to the TCE plume at TAN (data from Knobel et al., 1992). Total DIC was assumed to be the measured HCO_3^- and the pe of the system was specified by DO content. Model results were considered to be valid if overall electrical charge balance was $< 5\%$. Calculated saturation indexes (SI) for calcite in the TAN area range from 0.2 to 0.5, which suggest that calcite is slightly supersaturated within the TCE plume at TAN. It is significant to note that near the TAN disposal well at the center of the TCE plume that while DIC (and hence, calculated pCO_2 values) were elevated, so was the temperature (by up to 4°C) — resulting in roughly similar calcite SI values compared with wells away from the TAN disposal well. Wylie et al. (1999) suggest that the increased temperature at the disposal well reflects metabolic heat released by enhanced microbial activity; however, the alternative that "hot" sewage was pumped into disposal well at some point in the past cannot be discounted.

Another question that arises is if the bright luminescent calcite formed in association with microbial activity (either directly or indirectly), then what is the relationship between CO_2 mineralization and calcite formation? The observed abundance of bright luminescent calcite < 1–38 μg calcite/g total sample is low particularly when considering that this calcite was present in only 3 out of the 30 samples from TAN-37. Additionally, bright luminescent calcite is not present in samples from other boreholes. Fredrickson (unpublished data) determined bulk aerobic and anaerobic heteorotrophic microbial respiration on fresh basalt chips from multiple intervals at TAN-37. CO_2 mineralization rates range from 56 to 244 nmol of CO_2 g^{-1} $year^{-1}$. If this rate has been constant over the 45-year period (1952–1997), and assuming that all of this respired CO_2 has been incorporated into calcite, then 250–1100 μg calcite would potentially have been formed per g of sample. Calculated calcite formation based on CO_2 mineralization is significantly higher than the observed abundance of bright luminescent calcite. These results are consistent with previous studies in which in situ microbial activity measurements tend to overestimate biomass production (Chapelle and Lovley, 1990; Phelps et al., 1994).

8. Calcite as a proxy for redox status in contaminated aquifers

Zachara (1999) defines two categories of microbial mineralization (microbial directed, microbial driven). Microbial directed mineralization involves the formation of mineral products that confer an ecological advantage to an microorganism (Phoenix et al., this volume). Microbial driven mineralization is associated with biological activity that indirectly modulates geochemical conditions resulting in mineral formation (Zachara, 1999). Note that the sites of microbial-driven precipitation need not be in direct physical contact with the metabolically active microorganisms. A third category, microbially-influenced mineralization, defined here as microbial activity that does not actually facilitate mineral formation but does impart a geochemical signature on to abiotic precipitates.

This study does not attempt to establish a direct linkage between epicellular calcite precipitation and microbial activity. Instead it is our goal to establish that by either direct or indirect means microbial activity has imparted a recognizable signature into a calcite that can be related to the redox status within the SRPA at TAN. Two lines of evidence are generally used to establish a biotic connection in geochemical processes (Murphy and Schramke, 1998). These lines of evidence include the occurrence of microorganisms that utilize specific metabolic activities that can be linked to concentrations of aqueous species like Mn and Fe and the fractionation of stable isotopes that are indicative of overall biotic activity. The unconfined nature of the SRPA at TAN largely mutes the potential for variations in stable isotopes related to microbial activity as documented by the overall constancy of groundwater $\delta^{13}C$ of DIC measured from the TAN-33 borehole.

Several independent indicators indicate increased microbiological activity toward the center of the TCE plume at TAN. Basalt from the TAN-37 borehole, when compared with rock from other TAN boreholes (e.g., TAN-33) located more distally from the TAN Disposal Well, contained higher levels of culturable microorganisms, rates of aerobic and anaerobic acetate mineralization, and concentrations of extractable microbial DNA (Colwell, 1989; Colwell and Lehman, 1997; Palumbo et al. 1994; Lehman et al. 1998, 1999). Additionally, significant microbial iron reduction was noted in 75% of the cores obtained from TAN-37 vs. only 25% of the cores from TAN-33; a finding consistent with the decreased DO content of TAN-37 vs. TAN-33 groundwater. While enrichments for Mn reducing bacteria were not completed it is commonly recognized that iron-reducing bacteria are capable of also using oxidized Mn as a terminal electron acceptor (e.g., Loveley and Goodwin, 1988).

The above evidence does not conclusively demonstrate a microbial connection to the elevated Mn values of the bright luminescent distal tips. However, injection of TCE and sewage has certainly simulated microbial activity around the TAN injection well relative to ambient conditions in the SRPA. Consequently, it would seem dubious to advance a purely inorganic mechanism to explain the elevated Mn content of distal tip calcite. Whether the significant Mn present in TAN groundwater (and distal tip calcite) are due to microbial reduction of Mn-bearing minerals coupled with oxidation of organic matter (e.g., Lovely, 1991), reflect inorganic alteration of silicates (pyroxene) or Mn oxyhydroxides (Stumm and Morgan, 1981) in a setting where oxygen was locally depleted by microbial activity, or both is not determinable at present.

It is conceivable that such an approach could be applied to recently formed calcite (either naturally formed or artificially induced) present in other groundwater systems that have distinct redox zonations. Significantly, the minor element geochemistry of recently formed calcite have the potential to provide a proxy record for variations in redox zonation associated with successional changes in terminal electron acceptor utilization within subsurface microbial communities. Possible applicable sites span local, unconfined flow systems (e.g., oil spill at Bemidji, MN; Hiebert, 1994; leachate down gradient from landfill at Grindsted, Denmark; Bjerg et al., 1995) to regional flow systems that exhibits progressive depletion of potential electron acceptors (O_2, Fe^{3+}, SO_4^{2-}, and CH_4) along a flowpath (e.g., Middendorf aquifer, SC; Murphy and Schramke, 1998). Additionally, such criteria may be of potential use in the recognition of microbially-influenced carbonate from rocks whose geologic history is not well constrained (e.g., SNC meteorites; rocks from the Martian sample return mission).

9. Summary

Most calcite cement present in the ESRP aquifer at TAN is ancient in origin. However, the distal tips of the last calcite cement generation are brightly luminescent and have elevated Mn content. Given the history of this region, it is probable that the formation of the distal tips was the result of localized oxygen consumption associated with injection of organic contaminates starting in the 1950s.

Acknowledgements

This research is supported by a grant from the Environmental Science Management Program DE-AC07-76IDO1570 from the Department of Energy (DOE) to F.S. Colwell with additional support from DOE grant DE-FG02-94ER61821 to T.C.O. The authors are grateful for the assistance rendered by E. Vicenzi at the Princeton Material Institute and J. Fredrickson at Pacific Northwest National Laboratory.

References

Amieux, P., Bernier, P., Dalongeville, R., de Medwecki, V., 1989. Cathodoluminescence of carbonate-cemented Holocene beachrock from the Togo coastline (West Africa): an approach to early diagenesis. Sediment. Geol. 65, 262–272.

Amy, P.S., Haldeman, D.L., 1997. The Microbiology of the Terrestrial Deep Subsurface. Lewis Publishers, NY, p. 366.

Anderson, S.R., Bowens, B., 1995. Stratigraphy of the undersaturated zone and uppermost part of the Snake River plain aquifer at Test Area North, Idaho National Engineering Laboratory, Idaho. U.S. Geological Survey Water-Resources Investigation Report 95-4130. 47 pp.

Bjerg, P.L., Rugge, K., Pedersen, J.K., Christensen, T.H., 1995. Distribution of redox-sensitive groundwater quality parameters downgradient of a landfill (Grindsted, Denmark). Environ. Sci. Technol. 29, 1387–1394.

Chapelle, F.H., Lovley, D.R., 1990. Rates of microbial activity in deep coastal plain aquifers. Appl. Environ. Microbiol. 56, 1865–1874.

Coleman, M.L., Hedrick, D.B., Lovley, D.R., White, D.C., Pye, K., 1993. Reduction of Fe(III) in sediments by sulphate-reducing bacteria. Nature 361, 436–438.

Colwell, F.S., 1989. Microbiological comparison of surface soil and unsaturated subsurface soil from a semiarid high desert. Appl. Environ. Microbiol. 55, 2420–2423.

Colwell, F.S., Lehman, R.M., 1997. Carbon source utilization profiles for microbial communities from hydrologically distinct zones in a basalt aquifer. Microb. Ecol. 33, 240–251.

Conrad, M.E., DePaolo, D.J., Kennedy, B.M., Miller, E.C., 1997. Carbon isotope evidence for degradation of mixed contaminants in the vadose zone. Abstr. Programs — Geol. Soc. Am. 29, 186.

Dromgoole, E.L., Walter, L.M., 1990. Iron and manganese incorporation into calcite: effects of growth kinetics, temperature and solution chemistry. Chem. Geol. 81, 311–336.

Hiebert, F.K., 1994. Microbial diagenesis in terrestrial aquifer conditions: laboratory and field studies. PhD Dissertation, University of Texas at Austin, 204 pp.

Hiebert, F.K., Bennett, P.C., 1992. Microbial control of silicate weathering in organic-rich ground water. Science 258, 278–281.

Hendry, J.P., 1993. Calcite cementation during bacterial manganese, iron and sulphate reduction in Jurassic shallow marine carbonate. Sedimentology 40, 87–106.

Hendry, J.P., Ditchfield, P.W., Marshall, J.D., 1995. Two-stage neomorphism of Jurassic aragonitic bivalves: implications for early diagenesis. J. Sediment. Res.A 65, 214–224.

James, N.P., Choquette, P.W., 1984. Diagenesis 9 — limestones — the meteoric diagenetic environment. Geosci. Can. 11, 161–194.

Kaminsky, J.F., Keck, K.N., Schafer-Perini, A.L., Hersley, C.F., Smith, R.P., Stormberg, G.J., Wylie, A.H., 1994. Remedial Investigation Final Report with Addenda for the Test Area North Groundwater Operable Unit 1-07B at the Idaho National Engineering Laboratory. Idaho National Engineering Laboratory, Idaho Falls, ID, EGG-ER-10643.

Knobel, L.L., Bartholomay, R.C., Cecil, L.D., Tucker, B.J., Werner, S.J., 1992. Chemical constituents in the dissolved and suspended fractions of ground water from selected sites, Idaho National Engineering Laboratory and Vicinity, Idaho, 1989. U.S. Geol. Surv. Open-File Rep.92-51 Idaho National Engineering Laboratory, Idaho Falls, ID, 59 pp., DOE/ID-2210110643.

Lamphere, M.A., Kuntz, M.A., Champion, D.E., 1994. Petrography, age, and paleomagnetism of basalt lava flows in coreholes Well 80. U.S. Geol. Surv. Open-File Rep.93-327 Idaho National Engineering Laboratory, 40 pp., NRF 89-04, NRF 89-05, and ICP 123.

Lehman, R.M., Colwell, F.S., Smith, R., Delwiche, M., Fredrickson, J.K., Kieft, T., Phelps, T.J., White, D.C., 1998. Alteration of the microbial ecology of a fractured basalt aquifer by contaminants. Abstract from the 98th General Meeting of the American Society for Microbiology, May 1998, Atlanta, GA, USA.

Lehman, R.M., Colwell, F.S., Smith, R., Delwiche, M., O'Connell, S.P., Fredrickson, J.K., Brockman, F., Reysenbach, A.-L., Kieft, T., Phelps, T.J., Ringelberg, D.B., White, D.C., 1999. Longitudinal and vertical variations in the microbial ecology of a fractured basalt aquifer with respect to a contaminant plume. Abstract from the 4th International Symposium on Subsurface Microbiology, August 1999, Vail, CO, USA.

Lovely, D.R., 1991. Dissimilatory Fe and Mn reduction. Microbiol. Rev. 55, 259–287.

Lovely, D.R., Goodwin, S., 1988. Hydrogen concentrations as an indicator of the predominant terminal electron-accepting reactions in aquatic sediments. Geochim. Cosmochim. Acta 52, 2993–3003.

Machel, H.G., Mason, R., Mariano, A.N., Mucci, A., 1991. Causes and emission of luminescence in calcite and dolomite. In: Barker, C.E., Kopp, O.C. (Eds.), Luminescence Microscopy: Quantitative and Qualitative Aspects. Society of Economic Paleontologist and Mineralogists, Dallas, pp. 9–25, Short Course 25.

Mann, L.J., Knobel, L.L., 1987. Purgeable organic compounds in ground water at the Idaho National Engineering Laboratory, Idaho. U.S. Geol. Surv. Open-File Rep.87-766, 23 pp.

McMahon, P.B., Williams, D.F., Morris, J.T., 1990. Production and isotopic composition of bacterial CO_2 in deep coastal-plain sediments of South Carolina. Ground Water 28, 693–702.

Murphy, E.M., Schramke, J.A., 1998. Estimation of microbial respiration rates in groundwater by geochemical modeling constrained with stable isotopes. Geochim. Cosmochim. Acta 62, 3395–3406.

Palumbo, A.V., McCarthy, J., Parker, A., Pfiffner, S., Colwell, F.S., Phelps, T.J., 1994. Potential for microbial growth in arid subsurface sediments. Appl. Biochem. Biotechnol. 45–46, 823–834.

Phelps, T.J., Pfiffner, S.M., Sargent, K.A., White, D.C., 1994. Factors influencing the abundance and metabolic capacities of microorganisms in eastern coastal plain sediments. Microb. Ecol. 28, 351–364.

Phoenix et al. (this volume).

Pigott, J.D., Land, L.S., 1986. Interstitial water chemistry of Jamaican Reef sediment: sulfate reduction and submarine cementation. Mar. Chem. 19, 355–378.

Rightmire, C.T., Lewis, B.D., 1987. Hydrogeology and geochemistry of the unsaturated zone. USGS Water-Resources Investigations Report 87-41988. Radioactive Waste Management Complex, Idaho National Engineering Laboratory, ID, 90 pp.

Romanek, C.S., Grossman, E.L., Morse, J.W., 1992. Carbon isotopic fractionation in synthetic aragonite and calcite; effects of temperature and precipitation rate. Geochim. Cosmochim. Acta 56, 419–430.

Sansone, F.J., Tribble, G.W., Andrews, C.C., Chanton, J.P., 1990. Anaerobic diagenesis within recent Pleistocene, and Eocene marine carbonate frameworks. Sedimentology 37, 997–1009.

Savard, M.M., Veizer, J., Hinton, R., 1995. Cathodoluminescence at low Fe and Mn concentrations: a SIMS study of zones in natural calcite. J. Sediment. Res.A 65, 208–213.

Sippel, R.F., Glover, E.D., 1965. Structures in carbonate rocks made visible by luminescence petrography. Science 150, 732–739.

Sorenson, K.S., Peterson, L.N., Ely, R.L., 1999. Enhanced reductive dechlorination of TCE in a basalt aquifer. In: Leeson, A., Alleman, B.C. (Eds.), Engineered Approaches for In Situ Bioremediation of Chlorinated Solvent Contamination (A.). Battelle Press, Columbus, OH, pp. 147–155.

Stumm, W., Morgan, J.J., 1981. Aquatic Chemistry: an Introduction Emphasizing Chemical Equilibria in Natural Waters. Wiley, NY, 780 pp.

Tobin, K.J., Walker, K.R., Srinivasan, K., Steinhauff, D.M., 1996. Suboxic to anoxic diagenesis of platform-marginal ooids and bladed-to-fibrous calcite from the Middle Ordovician Ottosee Formation (East Tennessee). Geol. Soc. Am. Bull. 108, 155–167.

Tribble, G.W., 1993. Organic matter oxidation and aragonite diagenesis in a coral reef. J. Sediment. Petrol. 63, 523–527.

Vasconcelos, C., McKenzie, J.A., Bernasconi, S., Grujic, D., Tien, A.J., 1995. Microbial mediation as a possible mechanism for natural dolomite formation at low temperature. Nature 377, 220–222.

Wood, W.W., Low, W.H., 1986. Aqueous geochemistry and diagenesis in the eastern Snake River Plain aquifer system, Idaho. Geol. Soc. Am. Bull. 97, 1456–1466.

Wylie, A., Ralston, D., Johnson, G., Twining, B., 1999. Bioremediation of a contaminated basalt aquifer. Presented the 5th International Symposium on In Situ and On-Site Bioremediation, San Diego, CA.

Zachara, J., 1999. Biomineralization processes associated with iron reducing bacteria and implications to trace element cycling. Abstract from the 4th International Symposium on Subsurface Microbiology, August 1999, Vail, CO, USA.